Gradual loss of polarization in light scattered from rough surfaces: Electromagnetic prediction

Myriam Zerrad,* Jacques Sorrentini, Gabriel Soriano, and Claude Amra

Institut Fresnel, UMR CNRS6133 Aix-Marseille Universités, Ecole Centrale Marseille, Faculté des Sciences et Techniques de Saint Jérôme, 13397 Marseille Cedex 20, France
**myriam.zerrad@fresnel.fr*

Abstract: Electromagnetic theory is used to calculate the gradual loss of polarization in light scattering from surface roughness. The receiver aperture is taken into account by means of a multiscale spatial averaging process. The polarization degrees are connected with the structural parameters of surfaces.

OCIS codes: (260.5430) Polarization; (290.5855) Scattering, polarization; (030.5770) Roughness.

References and links

1. J. W. Goodman, *Statistical Optics* (Wiley Classic Library, 1985).
2. L. Mandel, and E. Wolf, eds., *Optical Coherence and Quantum Optics* (Cambridge University Press 1995).
3. J. W. Goodman, *Speckle Phenomena in Optics: Theory and Applications* (Roberts and Company Publishers, 2007).
4. M. E. Knotts, and K. A. O'Donnell, "Multiple scattering by deep perturbed gratings," J. Opt. Soc. Am. A **11**(11), 2837–2843 (1994).
5. E. Wolf, "Unified theory of Coherence and polarization of random electromagnetic beams," Phys. Lett. A **312**(5-6), 263–267 (2003).
6. C. Brosseau, "Polarization and Coherence Optics: Historical Perspective, Status and Future Directions," presented at the Frontiers in Optics, 2008.
7. E. Wolf, ed., *Introduction to the Theory of Coherence and Polarization of Light* (Cambridge University Press, 2007).
8. P. Réfrégier, and F. Goudail, "Invariant degrees of coherence of partially polarized light," Opt. Express **13**(16), 6051–6060 (2005).
9. J. Ellis, and A. Dogariu, "Complex degree of mutual polarization," Opt. Lett. **29**(6), 536–538 (2004).
10. C. Amra, M. Zerrad, L. Siozade, G. Georges, and C. Deumié, "Partial polarization of light induced by random defects at surfaces or bulks," Opt. Express **16**(14), 10372–10383 (2008).
11. J. Broky, J. Ellis, and A. Dogariu, "Identifying non-stationarities in random EM fields: are speckles really disturbing?" Opt. Express **16**(19), 14469–14475 (2008).
12. J. Li, G. Yao, and L. V. Wang, "Degree of polarization in laser speckles from turbid media: implications in tissue optics," J. Biomed. Opt. **7**(3), 307–312 (2002).
13. J. Sorrentini, M. Zerrad, and C. Amra, "Statistical signatures of random media and their correlation to polarization properties," Opt. Lett. **34**(16), 2429–2431 (2009).
14. D. Colton, and R. Kress, *Integral Equations methods in Scattering Theory* (New-York, 1983).
15. S. G. Hanson, and H. T. Yura, "Statistics of spatially integrated speckle intensity difference," J. Opt. Soc. Am. A **26**(2), 371–375 (2009).
16. L. Tsang, J. A. Kong, and K.-H. Ding, *Scattering of electromagnetic waves: numerical simulations*, Wiley series in remote sensing (Wiley-Interscience, 2001).

1. Introduction

Partial polarization of light has been the focus of numerous studies for decades [1–4], with numerous efforts still active in the field [5–10]. It is based on the concept of mutual coherence μ between the polarization modes of light, connected with a time average process of a cross-correlation term at space location **ρ**:

$$\mu(\boldsymbol{\rho}) = \frac{1}{\alpha}\left\langle E_S\left(\boldsymbol{\rho},t\right)E_P\left(\boldsymbol{\rho},t\right)\right\rangle_t \tag{1a}$$

#128675 - $15.00 USD Received 18 May 2010; accepted 24 Jun 2010; published 12 Jul 2010

with α the normalization coefficient:

$$\alpha^2 = \left\langle \left| E_S\left(\boldsymbol{\rho},t\right)\right|^2 \right\rangle_t \left\langle \left| E_P\left(\boldsymbol{\rho},t\right)\right|^2 \right\rangle_t \qquad \Rightarrow \quad \left|\mu\right| \le 1 \tag{1b}$$

and E_S, E_P the real polarization modes, $\langle\rangle_t$ an average process over time parameter t. Here mutual coherence is a time constant due to the value of optical frequencies in the visible regime, in regard to detector band-passes. Notice that Eq. (1) is for a single realization of the process $E_{SorP}(\boldsymbol{\rho},t)$ under study [7].

More recently a unified approach [5] was built to predict the capacity of polarization modes to interfere at different locations of space, depending on the former properties of the light source:

$$\mu(\boldsymbol{\rho}_1,\boldsymbol{\rho}_2) = \frac{1}{\alpha_{12}} \left\langle E_S\left(\boldsymbol{\rho}_1,t\right) E_P\left(\boldsymbol{\rho}_2,t\right) \right\rangle_t \tag{2a}$$

$$\text{with} \quad \alpha_{12}{}^2 = \left\langle \left| E_S\left(\boldsymbol{\rho}_1,t\right)\right|^2 \right\rangle_t \left\langle \left| E_P\left(\boldsymbol{\rho}_2,t\right)\right|^2 \right\rangle_t \tag{2b}$$

Coherence and polarization may also be gathered when a time delay τ is introduced between the fields [2,7], that is:

$$\mu(\boldsymbol{\rho}_1,\boldsymbol{\rho}_2,\tau) = \frac{1}{\alpha_{12}} \left\langle E_S\left(\boldsymbol{\rho}_1,t\right) E_P\left(\boldsymbol{\rho}_2,t-\tau\right) \right\rangle_t \tag{3a}$$

$$\text{with} \quad \alpha_{12}{}^2 = \left\langle \left| E_S\left(\boldsymbol{\rho}_1,t\right)\right|^2 \right\rangle_t \left\langle \left| E_P\left(\boldsymbol{\rho}_2,t-\tau\right)\right|^2 \right\rangle_t \tag{3b}$$

From these starting parameters a matrix formalism can be developed [2,7] to connect the depolarization of light with a temporal average process over the product of polarization modes.

However alternative situations exist when light originates from the scattering of a random medium illuminated with monochromatic and fully polarized light. Due to the illumination conditions, the temporal average process vanishes but for most scattering samples light is still said to be not polarized, and experiment does not reveal polarized interferences. Such result is due to the angular behavior (amplitude and phase) of the scattering coefficients that strongly vary from one direction to another in the far field speckle pattern. Depending on the angular correlation between the polarization modes and its derivatives, polarization of light may appear to be spatially randomized at the speckle scale. In other words, because most detectors collect millions of speckle grains of different polarization states within their angular aperture, the resulting output signal is an average process that cancels any interference pattern when superposing the modes with retardation and analyzer plates. Hence light is depolarized but the nature of this depolarization is specific of a spatial or angular average process that retained less studies [11–13] until now. Moreover, this depolarization is aperture dependent and requires a multi-scale investigation [11–13].

The scope of this paper is to discuss the progressive depolarization of light in such a spatial average process. From one regime (fully polarized) to another (depolarized), the transition is connected with the microstructure of the scattering samples. These samples are rough surfaces, for which reason depolarization can be said “roughness-induced”. All calculation is based on the integral method [14] that was largely used in electromagnetic optics. Depending on the surface parameters, the polarization transition is more or less abrupt, and the multi-scale analysis allows us to predict the aperture range where full polarization can be recovered.

#128675 - $15.00 USD Received 18 May 2010; accepted 24 Jun 2010; published 12 Jul 2010

2. Multi-scale analysis of polarization

Consider a scattering sample under monochromatic and fully polarized illumination. We now use complex notations for the electromagnetic field. The temporal average vanishes and mutual coherence is turned into a single field product at locations $\boldsymbol{\rho}_1$ and $\boldsymbol{\rho}_2$, that is:

$$\mu(\boldsymbol{\rho}_1,\boldsymbol{\rho}_2)=\frac{E_S\left(\boldsymbol{\rho}_1\right)E_P^{\ *}\left(\boldsymbol{\rho}_2\right)}{\sqrt{\left|E_S\left(\boldsymbol{\rho}_1\right)\right|^2\left|E_P\left(\boldsymbol{\rho}_2\right)\right|^2}}\qquad\Rightarrow\quad\left|\mu\right|=1 \tag{4}$$

Equation (4) relates the fact that light scattering is fully polarized at any location of space, as predicted by Maxwell solutions in the far field (plane waves). However any detector will integrate the signal over its angular aperture or solid angle $\Delta\Omega$, so that Eq. (4) must be rewritten, if we restrict ourselves to the case of a single space location ($\boldsymbol{\rho}_1 = \boldsymbol{\rho}_2 = \boldsymbol{\rho}$), as:

$$\mu(\boldsymbol{\rho},\Delta\Omega)=\frac{\left\langle E_S\left(\boldsymbol{\rho}\right)E_P^{\ *}\left(\boldsymbol{\rho}\right)\right\rangle_{\Delta\Omega}}{\alpha} \tag{5a}$$

$$\text{with:}\quad\alpha^2=\left\langle\left|E_S\left(\boldsymbol{\rho},\Delta\Omega\right)\right|^2\right\rangle_{\Delta\Omega}\left\langle\left|E_P\left(\boldsymbol{\rho},\Delta\Omega\right)\right|^2\right\rangle_{\Delta\Omega} \tag{5b}$$

At this step Eq. (5) is the starting point to redevelop the matrix formalism [2,7] with strong analogies with the classical definition of the degree of polarization (DOP) which is a more directly measurable quantity [3,7]. The results are the following:

$$MDOP(\rho,\Delta\Omega)=\sqrt{1-4\frac{\det\left\{J\left(\rho,\Delta\Omega\right)\right\}}{\left[tr\left\{J\left(\rho,\Delta\Omega\right)\right\}\right]^2}} \tag{6}$$

where MDOP is the multi-scale degree of polarization calculated with solid angle $\Delta\Omega$ around point $\boldsymbol{\rho}$, and J the coherence matrix:

$$J(\rho,\Delta\Omega)=\begin{pmatrix}\left\langle\left(E_S\right)^*E_S\right\rangle_{\Delta\Omega} & \left\langle\left(E_S\right)^*E_P\right\rangle_{\Delta\Omega}\\ \left\langle\left(E_P\right)^*E_S\right\rangle_{\Delta\Omega} & \left\langle\left(E_P\right)^*E_P\right\rangle_{\Delta\Omega}\end{pmatrix} \tag{7}$$

We first notice a key difference due to the aperture influence, and that the MDOP differs from the spatial average of the local DOP, that is:

$$MDOP(\rho,\Delta\Omega)\neq\left\langle DOP(\rho)\right\rangle_{\Delta\Omega} \tag{8}$$

with $\left\langle DOP(\rho)\right\rangle_{\Delta\Omega}=DOP(\rho)=1$ due to the illumination conditions. Moreover, evidence is that the MDOP and DOP are identical for a null aperture, that is:

$$MDOP(\rho,\Delta\Omega=0)=DOP(\rho)=1 \tag{9}$$

A multi-scale investigation is now required to go further; such analysis was not necessary in the temporal average process, due to the value of optical frequencies in regard to detector band-passes. However in the spatial average process mutual coherence is now driven by the crossed fluctuations of the polarization fields within the receiver aperture. Depending on the scattering sample and its microstructure, these fluctuations may be severe or not, correlated or not.... Hence the MDOP may take unity or zero values depending on the scattering centers and the receiver aperture. Equations (6) and (7) predict the MDOP to be unity (MDOP = 1) at the speckle size, and less than unity (MDOP < 1) at larger integration areas. Finally the derivative of the MDOP curve depends on the surface parameters which control the gradual transition between two extreme states of light polarization (MDOP = 1 and MDOP close to 0).

#128675 - $15.00 USD Received 18 May 2010; accepted 24 Jun 2010; published 12 Jul 2010

3. Electromagnetic prediction

The simulations of statistical parameters such as the preceding MDOP are classically achieved using the Goodman models [3] of either partially or fully developed speckle. The simplicity of those models enables ones to obtain in-depth analytical expressions [12,15]. In this paper we make no such approximation, relying on an electromagnetic model to quantify the MDOP. To investigate the depolarization process at different scattering regimes, the complex scattered fields must be perfectly known at all directions in the far field at a speckle size; for this reason the numerical approach has to be quite fast, and we restrict ourselves to the case of one dimensional surfaces z = h(x). Moreover, in order to cover most scattering regimes from perturbative roughnesses to the resonant domain, a rigorous solution of Maxwell's equations is required. Hence we used the Method of Moments based on the boundary integral approach [16] for rough profiles separating air and a metal with finite conductivity. Notice here that the metallic case gives more weight to multiple reflections at the surface, increasing the speed of depolarization process.

Phase and amplitude of the electromagnetic field scattered by a panel of arbitrary 1D surfaces were calculated for the two polarization modes S and P, where the electric (S) or the magnetic (P) field is along the invariant y-direction, with z the average surface normal. The surfaces are realizations of a stationary stochastic process with Gaussian height distribution as well as Gaussian autocorrelation function. As such, the roughnesses are entirely characterized from a statistical point-of-view by their height root mean square h_{rms} and their correlation length L_{cor}. A 6 mm-long profile is illuminated with a fully polarized Gaussian beam under normal incidence at 632.8nm wavelength. The profiles are assumed to be engraved in aluminum, of complex optical refractive index 1.39 + j 7.65 at this wavelength.

The complex polarized components A_S and A_P of the scattered field are calculated for 10000 scattering angles in the θ angular range (0°– 30°) and regularly sampled with a step of 5e-5rad, that is with δθ = 2.8e-3°. The angle runs from 0.6761° to 29.3239°, so that the specular region (θ = 0°) is avoided. Such an angular resolution permits us to precisely resolve the speckle, which is of characteristic size 1.15e-2° (= 2e-4 rad≈□/3mm = 2.11e-4) in this configuration. The profiles are generated using the spectral method [16]. Profiles are spatially sampled with a step that depends on the correlation length. It is set to 92nm for L_{cor} = 2μm and to 23nm when L_{cor} = 100nm.

Invariance of the surfaces in one direction is a severe assumption. In the paper's configuration, no cross-polarization is predicted in the plane of incidence, while it should appear for 2D roughness as soon as the perturbative regime is left. However, the Method of Moments gives the rigorous solution of a wave scattering problem, with all multiple interactions accurately taken into account, which is the point here.

In what follows we use the following notations:

$$\begin{aligned} A_S &= \sqrt{I_S}\; e^{j\delta_S} \\ A_P &= \sqrt{I_P}\; e^{j\delta_P} \\ \delta &= \delta_P - \delta_S \end{aligned} \tag{10}$$

with I_S and I_P the polarized speckle patterns and δ the polarimetric phase difference. We also use the amplitude or polarization ratio $\beta = (I_P/I_S)^{0.5} = |A_P/A_S|$.

3. The case of two extreme polarization regimes

In Figs. 1 and 2 we plotted the ratio $\beta = |A_P/A_S|$ and the polarimetric phase delay δ of the polarized speckles for two surfaces of strongly different topography. One surface is specific of the perturbative regime with parameters h_{rms} = 50 nm and L_{cor} = 2 μm, which implies a low quadratic slope ($s \approx h_{rms}/L_{cor}$ = 2.5%). On the other hand, the second surface has a significant slope (s ≈100%, h_{rms} = 100 nm and L_{cor} = 0.1 μm) and scatters the whole incident light.

#128675 - $15.00 USD Received 18 May 2010; accepted 24 Jun 2010; published 12 Jul 2010

350 data points are plotted in the angular range 10°-11°, that is $\Delta\Omega = 1°$. In Fig. 1 we observe super-imposition of the polarized speckles for the perturbative surface, since the curve exhibits slight departure from unity ($|A_P/A_S| \approx 1$); this is no more the case for the high slope surface which shows 2 decades fluctuations for the amplitude ratio ($|\beta_{max}/\beta_{min}| \approx 100$). Strong differences also appear when the phase data (Fig. 2) are considered: while the phase term remains close to $-\pi$ for the perturbative surface, it appears quasi-uniformly distributed within $\pm\pi$ for the other one. These results provide a preliminary signature to identify the scattering regime; in other words, a perturbative surface cannot depolarize light [3] Calculation of the MDOP within the receiver aperture $\Delta\Omega = 1°$ gives MDOP = 1 for the low slope surface, and MDOP = 0.3 for the other one.

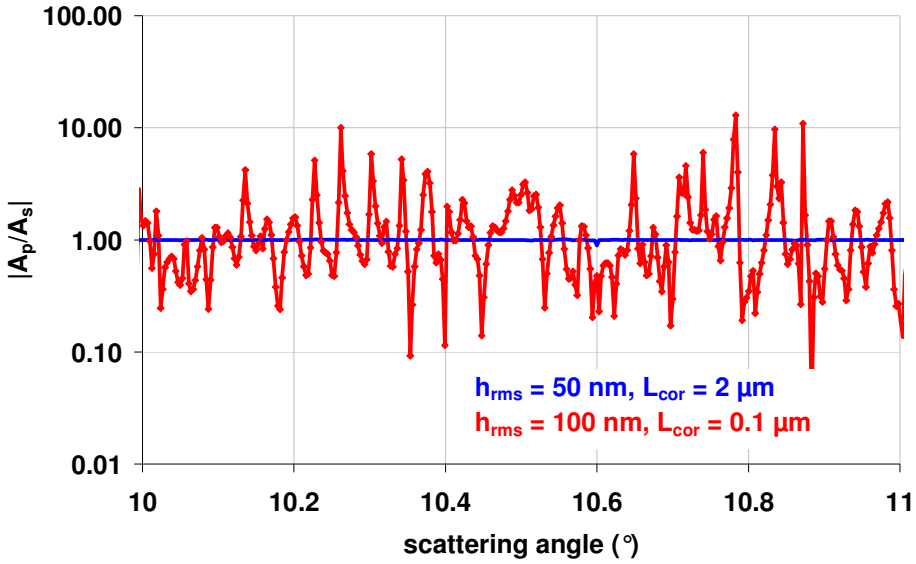

Fig. 1. Amplitude ratio $\beta = |A_P/A_S|$ of the scattered field for two surfaces whose definition parameters are $h_{rms} = 50$ nm, $L_{cor} = 2$ µm and $h_{rms} = 100$ nm, $L_{cor} = 0.1$ µm (see text).

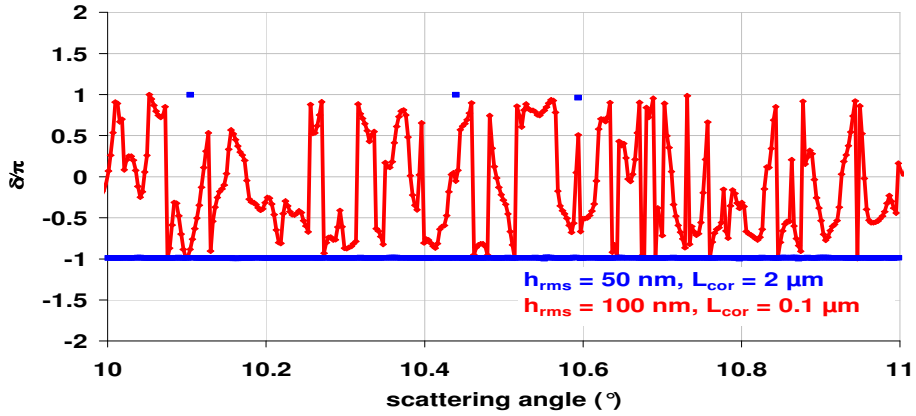

Fig. 2. Polarimetric phase delay δ of the scattered field for two surfaces whose definition parameters are $h_{rms} = 50$ nm, $L_{cor} = 2$ µm and $h_{rms} = 100$ nm, $L_{cor} = 0.1$ µm (see text).

Another way to emphasize these results can be found in the histograms of β and δ. In Fig. 3 it is shown how perturbative surfaces give β histograms that approach Dirac functions (narrow width) centered around unity; then the histogram width increases with slope, as well as asymmetry and departure from unity.

#128675 - $15.00 USD
Received 18 May 2010; accepted 24 Jun 2010; published 12 Jul 2010

Figure 4 is given for the δ histograms; similar results are obtained for perturbative surfaces (narrow peak at −180°), while higher slope surfaces give a uniform histogram in the interval.

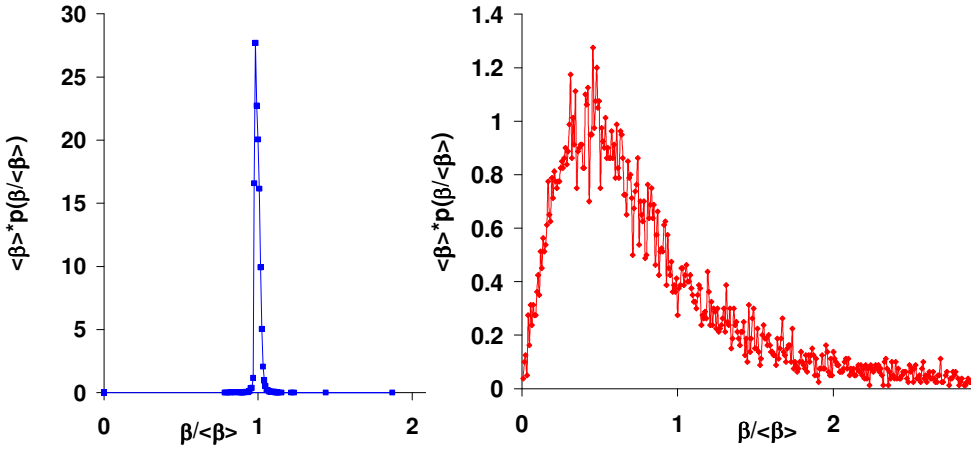

Fig. 3. Histogram of amplitude ratio $|A_P/A_S|$ of the scattered field for two surfaces whose definition parameters are h_{rms} = 50 nm, L_{cor} = 2 µm (left) and h_{rms} = 100 nm, L_{cor} = 0.1 µm (right).

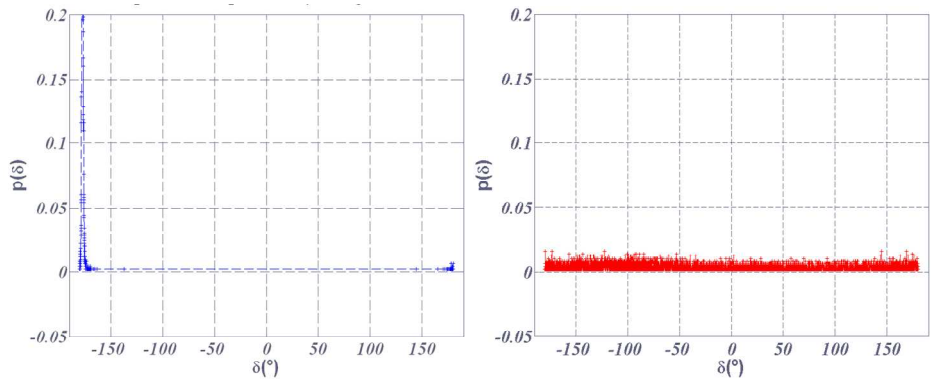

Fig. 4. Histogram of polarimetric phase delay δ of the scattered field for two surfaces whose definition parameters are h_{rms} = 50 nm, L_{cor} = 2 µm (right) and h_{rms} = 100 nm, L_{cor} = 0.1 µm (left).

4. Scan of surface parameters

In this section twelve surfaces of same correlation length (L_{cor} = 100nm) were considered. The roughness values h_{rms} vary from 1nm to 100nm, so that the slope is in the range (1%-100%). For each surface 350 data points were calculated in the angular range (10°-11°) and plotted on the Poincaré sphere. Results are given in Figs. 5 and 6. As predicted, low slope surfaces slighlty spread the polarization location over the sphere, which indicates that full polarization is globally maintained for these surfaces and similar to the incident polarization (linear 45°).

On the other hand higher slopes rapidly spread out the polarization over the sphere, and cover the whole sphere at high slopes. Because all these data points will be collected by the receiver aperture ΔΩ = 1°, the resulting polarization will be partial. Results are given in Fig. 6 for the MDOP(1°) that we plotted versus the surface slope. One may keep in mind that partial polarization falls to 0.84 for a 20% slope, with a minimum value at 0.3 when the slope is 100%. Higher slopes would create complete depolarization within ΔΩ, but our computer code is too much time consuming to explore this range.

#128675 - $15.00 USD Received 18 May 2010; accepted 24 Jun 2010; published 12 Jul 2010

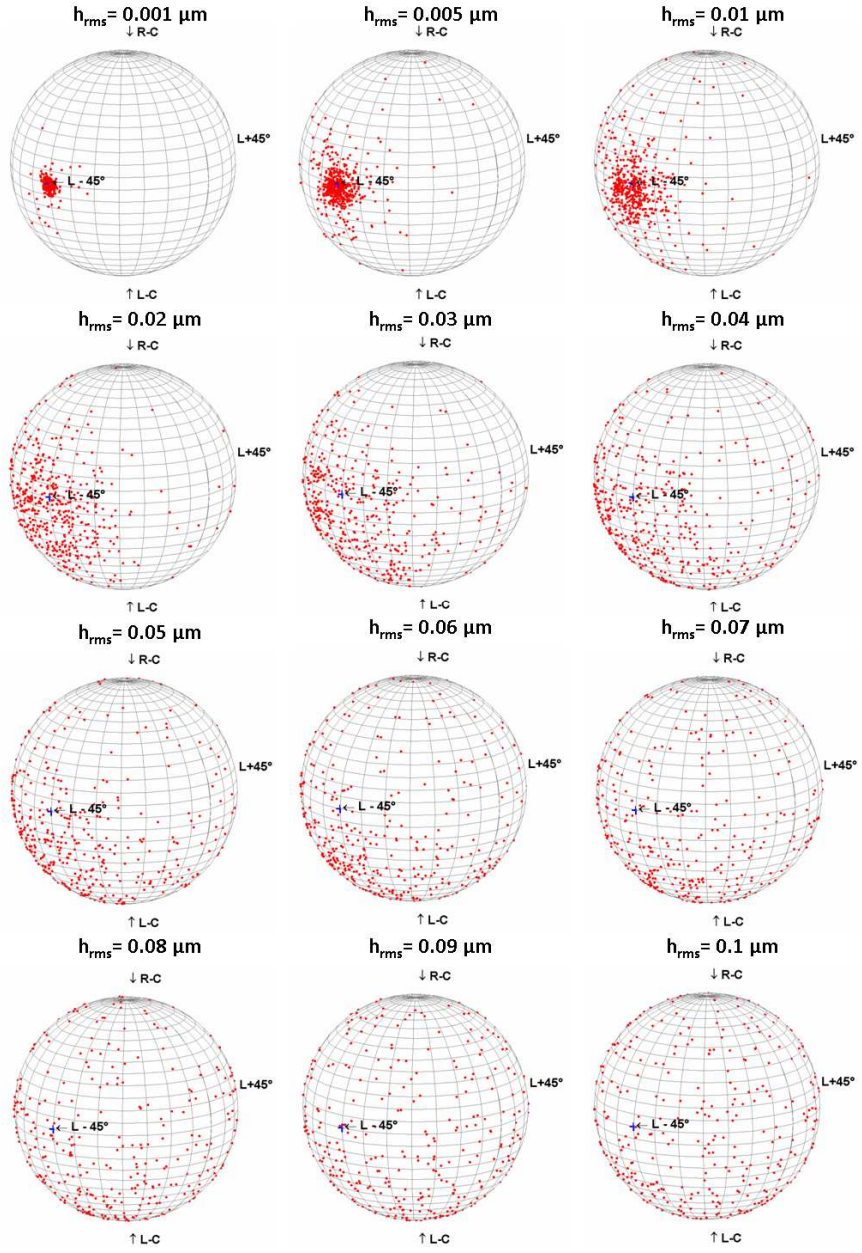

Fig. 5. Variation of the scattered polarization within 1° angular range (10°-11°), plotted on the Poincaré sphere for different surface slopes (1%-100%)-(R-C and L-C are the circular polarization states respectively right and left. L ± 45° is the linear ± 45° polarization state).

#128675 - $15.00 USD Received 18 May 2010; accepted 24 Jun 2010; published 12 Jul 2010

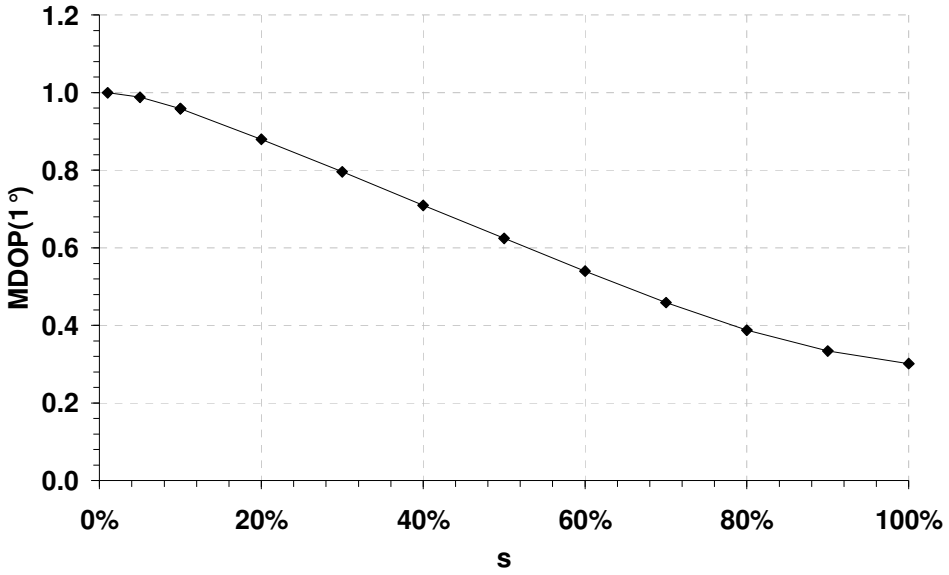

Fig. 6. MDOP(1°) plotted versus increasing surface slope s for L_{cor} = 0.1 µm.

5. Gradual transition and the MDOP function

Now we analyze the gradual transition of polarization from one regime to another. For this we have to calculate the multi-scale function MDOP ($\Delta\Omega$) for each of the preceding surfaces. However until now the spatial average was processed within the angular aperture $\Delta\Omega$ centered around the angle θ_0 = 10.5°, so that we studied the function MDOP (θ_0 = 10.5°, $\Delta\Omega$). In what follows 3 values are considered for θ_0, that are 10°, 10.5° and 11°. In all cases the maximum aperture is 1° apart from this average angle θ_0.

The MDOP (θ_0, $\Delta\Omega$<1°) functions are plotted in Fig. 7 versus the coherence areas or speckle grains; each coherence area is about 5 data points so that 40 coherence areas are enough to cover a 0.5° aperture, which is enough to approach the asymptotic behavior. The first figures just confirm that perturbative surfaces keep full polarization whatever the angular aperture lower than 1°. When the slope increases, we first observe, for a given average θ_0 angle, fluctuations of polarization versus the aperture; hence the curves are not monotonic and one may measure a slight "re-polarization" when increasing the aperture, and this local re-polarization is specific of the θ_0 angle.

#128675 - $15.00 USD Received 18 May 2010; accepted 24 Jun 2010; published 12 Jul 2010

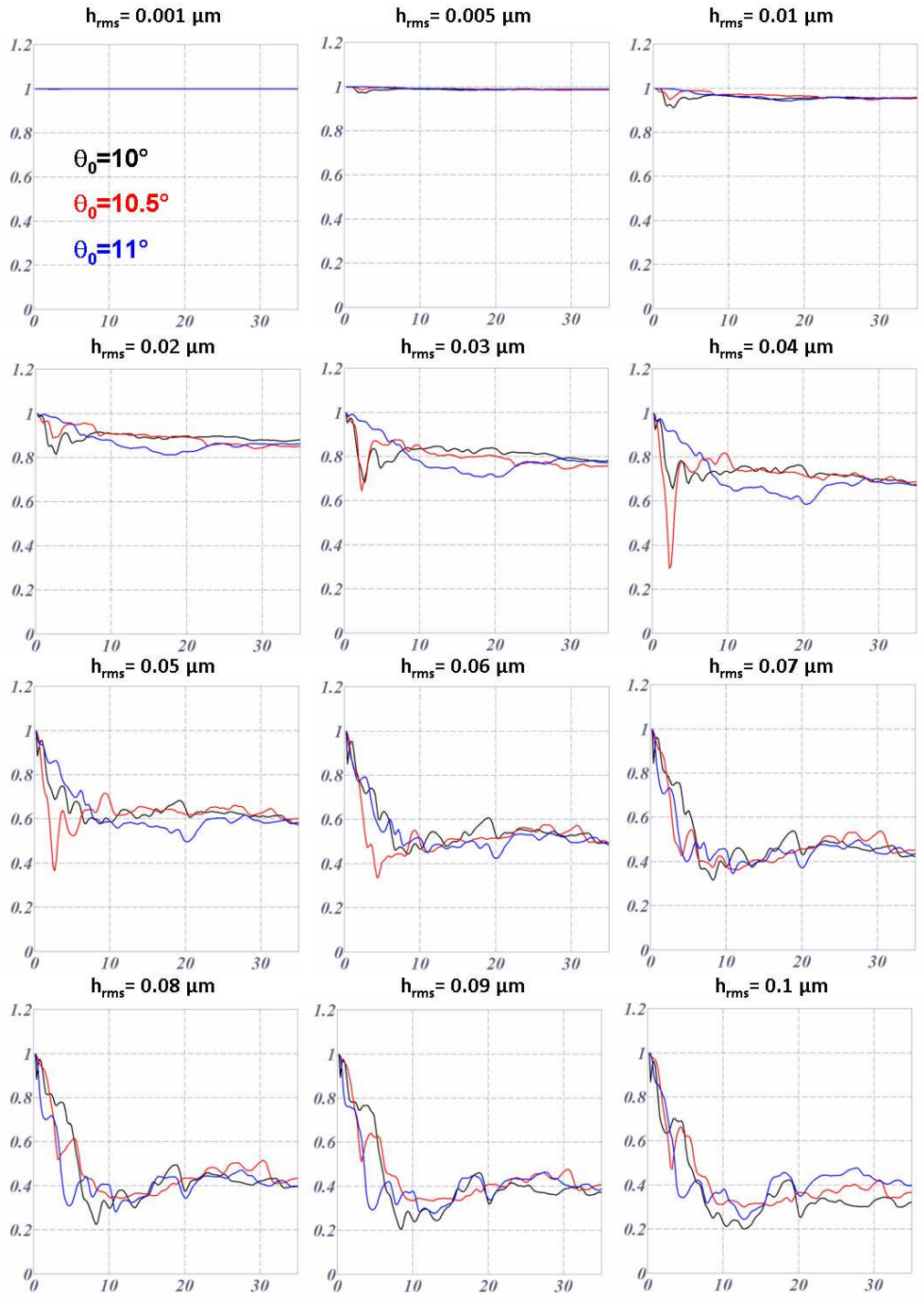

Fig. 7. MDOP function calculated versus number of coherence areas (see text) for different surface slopes. For each surface the MDOP is calculated for three different values of the average θ_0 angle (10, 10.5 and 11°)- see text.

#128675 - $15.00 USD Received 18 May 2010; accepted 24 Jun 2010; published 12 Jul 2010

Now to go further one may search for a MDOP function more closely related to the surface, with a reduced influence on θ_0. For this reason we considered the average value of the MDOP over the θ_0 angle, that is:

$$MDOP^{*}\left(\Delta\Omega\right) = \left\langle MDOP\left(\Delta\Omega, \theta_0\right)\right\rangle_{\theta_0} \tag{11}$$

With this average function all ripples are cancelled (Fig. 8) within the aperture range, since the result is a purely decreasing function of $\Delta\Omega$. It gives a global view of the speed at which polarization is lost. Moreover, it reveals a quasi-asymptotic value at $\Delta\Omega$ = 1°, that should represent the maximum depolarization obtained with such surfaces. In other words, the results indicate that surfaces with slopes lower than 100% cannot depolarize light at a value lower than 0.4. However strictly speaking one should scan all correlation lengths, while here we limit ourselves to L_{cor} = 100nm.

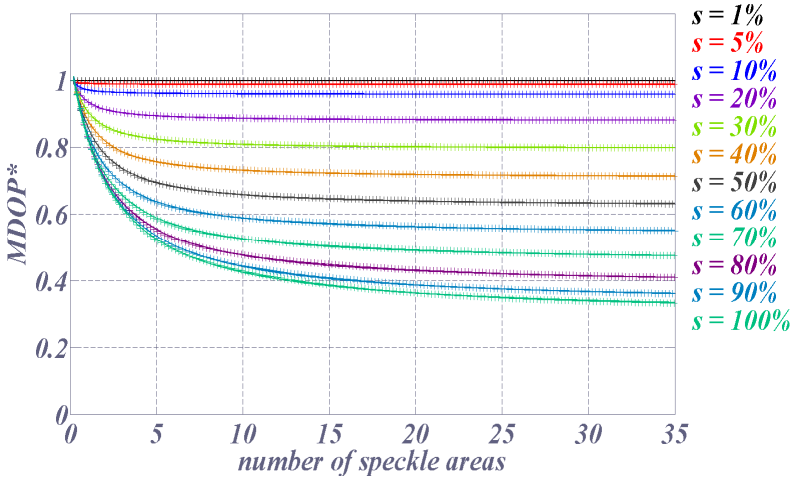

Fig. 8. Average MDOP* and its theoretical fit (f) as a function of the detector aperture for each of the 12 surfaces under study (see text). The fit is quasi perfect for each curve (MDOP* and fit are superimposed for each h_{rms}). The average is taken in the θ_0 range (0°-30°).

The shape of the curves also suggests to search for a fit of the form:

$$MDOP^{*} \approx f\left(\Delta\Omega\right) = a\left(b + \Delta\Omega\right)^{-n} + c \tag{12}$$

where parameter c gives the lower depolarization (asymptotic value of non perturbative surfaces), and $ab^n + c = 1$ for a unity DOP value at the origin, so, the fit parameter b can be deduced from a,c and n. Results are given in Fig. 8 and show a quasi perfect agreement between MDOP* and the fit f, since the two curves are superimposed whatever the surface.

#128675 - $15.00 USD Received 18 May 2010; accepted 24 Jun 2010; published 12 Jul 2010

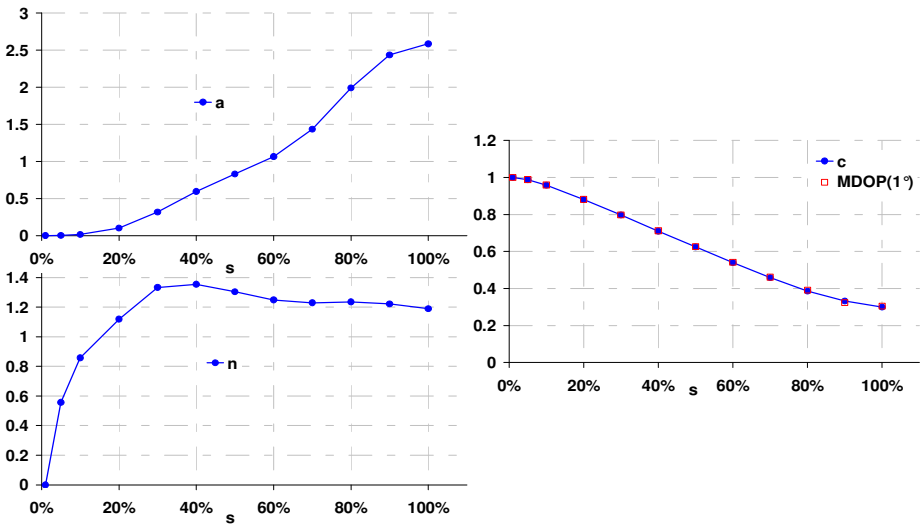

Fig. 9. Evolution of a, c and n the 3 MDOP* fit parameters theoretical versus surface slope s.

In Fig. 9 the fit parameters *a*, *c* and *n* are given versus the surface slopes, and parameter c is compared to MDOP(1°). As predicted, the asymptotic MDOP* is quasi-identical to this parameter. Moreover, the power parameter (n) rapidly reaches a stationary value of the order of 1.2.

6. DOP cartography versus slope and height

Until now we scanned the surfaces heights or slopes but we used the same correlation length L_{cor} = 0.1µm, which reduces our MDOP prediction to short correlation surfaces. For this reason the correlation length is now scanned with values in the range 0.1µm - 3µm. Results are plotted in Fig. 10, and consider the asymptotic MDOP value ($\Delta\Omega$ = 1°) versus both h_{rms} and L_{cor}. We observe at a constant roughness (vertical line) that the DOP increases up to 1 when the correlation length varies from 0.1 to 3 µm. Then at a constant correlation length (horizontal line), the DOP falls to zero when the roughness increases. Lastly, at a constant slope (oblique line) given by the L_{cor} /h_{rms} ratio, we notice in a first approximation that the MDOP remains quasi-constant; this last result emphasizes the key role of surface slope in the MDOP prediction.

#128675 - $15.00 USD Received 18 May 2010; accepted 24 Jun 2010; published 12 Jul 2010

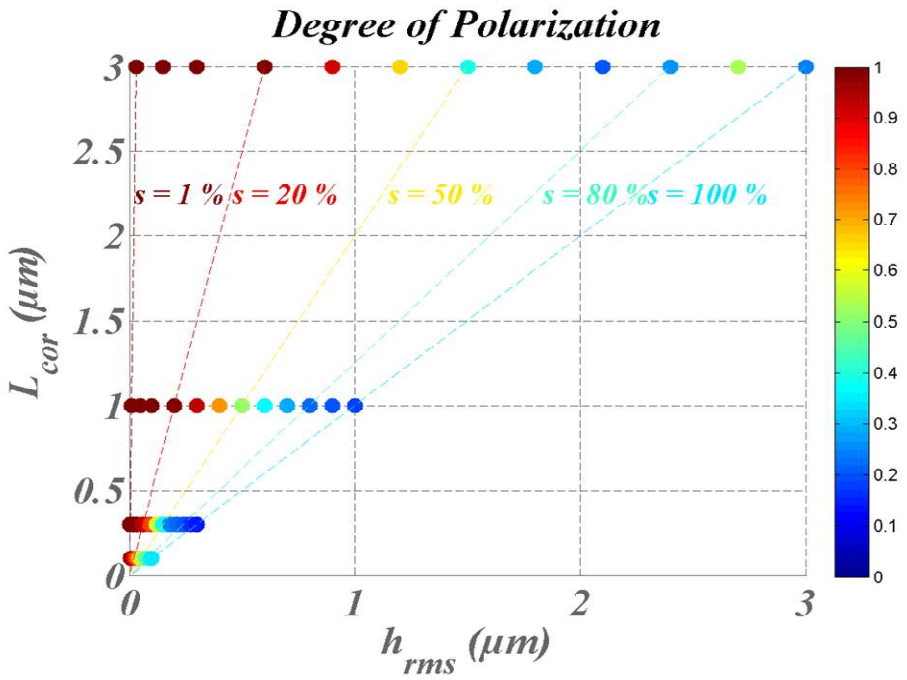

Fig. 10. MDOP(1°) levels versus roughness and correlation length.

7. Conclusion

An exact calculation method was used to predict the gradual loss of polarization induced by surface roughness in a spatial average process. The results allow to predict the depolarization efficiency of scattering samples versus their surface topography. While perturbative surfaces cannot depolarize light, surfaces with 100% slopes reduce polarization to a value close to DOP = 0.2 within a 1° detector aperture for Lcor = 0.3 µm. A multi-scale function (MDOP) was also calculated to analyze the DOP variations versus receiver aperture $\Delta\Omega$, which revealed a ripple in the calculation range. Also, averages values of the MDOP($\Delta\Omega$) were shown to exhibit power law behaviors that can be used as additional signatures of the samples topography. All results can be helpful to analyze or predict the optical contrast when polarized interferences are measured on light scattering within a particular solid angle.

#128675 - $15.00 USD Received 18 May 2010; accepted 24 Jun 2010; published 12 Jul 2010